Oxidative Addition to Cyclometalated Azobenzene Platinum(II) Complexes: A Route to Octahedral Liquid Crystalline Materials

Mauro Ghedini,* Daniela Pucci, Alessandra Crispini, and Giovanna Barberio

Dipartimento di Chimica, Università della Calabria, I-87030 Arcavacata (CS), Italy

Received September 29, 1998

The 4,4′-disubstituted azobenzene ligands HL^{a-d} react with $[(\eta^3\text{-}C_4H_7)Pt(\mu\text{-}Cl)]_2$ to give the dinuclear cycloplatinated complexes $[(L^{a-d})Pt(\mu\text{-}Cl)]_2$, which are easily converted to their mononuclear Pt(II) acetylacetonate derivatives $[(L^{a-d})Pt(acac)]$. Oxidative addition to the square-planar Pt(II) complexes $[(L^{a-d})Pt(acac)]$ of electrophilic substrates such as I_2 or CH_3I (RI) eventually led to the corresponding octahedral Pt(IV) $[(L^{a-d})Pt(acac)I_2]$ and $[(L^{a-d})Pt(acac)(CH_3)I]$ products. Characterization by X-ray crystallography on model complexes $[(L^a)Pt(acac)]$, $[(L^a)Pt(acac)I_2]$, and $[(L^a)Pt(acac)(CH_3)I]$ has been carried out, showing that the I_2 or CH_3I ligands are bound to the Pt(IV) center at the apical positions. The presence of two ligands in apical position led to the loss of the short intermolecular Pt- - -Pt distance of 3.311(1) Å observed in the square-planar complex $[(L^a)Pt(acac)]$. Thermotropic mesomorphism is observed for both the Pt(II) and Pt(IV) species with clearing temperatures, mainly lower than those of the corresponding organic ligands. These products are the first examples of Pt(IV) octahedral liquid crystalline species and suggest that oxidative addition to appropriate Pt(II) precursors should be a convenient synthetic procedure for new hexacoordinated Pt(IV) mesogenic materials.

Introduction

The metallomesogens[1] are metal-containing liquid crystalline materials whose chemical or physical properties can be fine-tuned by using the differences that each metal center bring about. The synthesis of metallorganic and coordination compounds that feature mesomorphism therefore represents a topic for material science.

Mesogenic coordination compounds involving transition metals are now widespread.[2] On the contrary, metallorganic species are less common, and the available data mainly concern cyclometalated Pd(II) imines or azobenzenes[3] and ferrocene derivatives.[4] Other complexes belonging to this class include some Pt(II) derivatives with the same ligands,[5] a few examples of Hg(II) orthometalated azobenzenes,[6] and Mn(I) or Re(I) cyclometalated imines.[7] With reference to the compounds where the metal is σ-bonded to a carbon atom, the metal center adopts a square-planar [Pd(II) and Pt(II)], trigonal planar [Hg(II)], and octahedral [Mn(I) and Re(I)] coordination geometry and gives rise to a five-membered metallacycle with a rodlike mesogenic ligand. Liquid crystalline metallorganic complexes have not yet been systematically explored, and further data are required to single out how the topology of the metal environment is related to the occurrence of thermotropic mesomorphism.

It has been observed that additional ligands placed out of the plane where the mesogenic ligand lies are beneficial in that they lower the transition temperatures and improve the thermal stability of the resulting mesophases.[5d,8] Both these aspects are of interest with reference to the processability of such materials, so that mesogenic octahedral complexes may be relevant for applicative purposes.

The only examples of hexacoordinated orthometalated liquid crystals reported up to now are mononuclear Mn(I) and Re(I) carbonyl complexes.[7] Unfortunately, these compounds require a rather involved synthetic strategy. Indeed, they have been obtained reacting the organic ligand with the unmodifiable, preexisting metal complex fragment (i.e., $[M(CO)_4]$, M = Mn, Re). Therefore more versatile synthetic pathways to prepare hexacoordinated metallomesogens are required.

Pt(II) chemistry is characterized by oxidative addition reactions,[9] and square-planar cycloplatinated species could become suitable starting materials for the synthesis of new octahedral Pt(IV) mesogens. In particular,

* Corresponding author. Fax: Int. code +(984)492044. E-mail: m.ghedini@unical.it.

(1) (a) Serrano, J. L. *Metallomesogens*; VCH: Weinheim, 1996. (b) Bruce, D. W. In *Inorganic Materials*, 2nd ed.; Bruce, D. W., O'Hare, D., Eds.; Wiley: Chichester 1996.

(2) Espinet, P.; Esteruelas, M. A.; Oro, L. A.; Serrano, J. L.; Sola. E. *Coord. Chem. Rev.* **1992**, *117*, 215.

(3) Hudson, S. A.; Maitlis, P. M. *Chem. Rev.* **1993**, *93*, 861.

(4) Deschenaux, R.; Goobdy, J. W. In *Ferrocenes*; Togni, A., Hayashi, T., Eds.; VCH: Weinheim, 1995; p 471.

(5) (a) Praefcke, K.; Bilgin, B.; Usol'tseva, N.; Heinrich, B.; Guillon, D. *J. Mater. Chem.* **1995**, *5*, 2257. (b) Buey, J.; Diez, L.; Espinet, P.; Kitzerow, H. S.; Miguel, J. A. *Chem. Mater.* **1996**, *8*, 2375. (c) Ortega, J.; Folcia, C. L.; Extebarria, J.; Ros, M. B.; Miguel, J. A. *Liq. Cryst.* **1997**, *23*, 285. (d) Ghedini, M.; Neve, F.; Pucci, D. *Eur. J. Inorg. Chem.* **1998**, 501.

(6) Omenat, A.; Ghedini, M. *J. Chem. Soc., Chem. Commun.* **1994**, 1309.

(7) (a) Bruce, D. W.; Liu, X. H. *J. Chem. Soc., Chem. Commun.* **1994**, 729. (b) Bruce, D. W.; Liu, X. H. *Liq. Cryst.* **1995**, *18*, 165.

(8) (a) Bruce, D. W. *Adv. Mater.* **1994**, *6*, 699. (b) Ghedini, M.; Pucci, D.; Neve, F. *Chem. Commun.* **1996**, 137.

(9) Anderson, G. K. In *Comprehensive Organometallic Chemistry*; Wilkinson, G., Stone, F. G. A., Abel, E. W., Eds.; Pergamon Press: 1995; Vol. 9.

10.1021/om9808155 CCC: $18.00
Publication on Web 05/04/1999

this approach could be very useful to devise an alternative strategy to design complexes easily modulated as far as the apical positions are concerned. The present work has been planned in order to test a synthetic procedure to obtain hexacoordinated Pt(IV) mesogens by oxidative addition to cyclometalated azobenzene Pt(II) complexes.

Orthoplatination, a reaction which for a long time was not readily accomplishable,[10] is now easily accessible through an elegant synthetic method[11] which involves the use of $[(\eta^3\text{-}C_3H_5)Pt(\mu\text{-}Cl)]_2$. The products obtained from the reaction of azobenzenes with di-μ-chlorobis(η^3-allylplatinum) or di-μ-chlorobis(η^3-2-methylallylplatinum) are dinuclear chloro-bridged cyclometalated complexes with a symmetric "H-shaped" molecular structure.[5b,d] With reference to the thermotropic properties, the structurally similar Pd(II) products usually display high transition temperatures. However, their mononuclear derivatives, obtained from a bridge-splitting reaction with a monoanionic chelating ligand such as acetylacetonate, are unsymmetric "P-shaped" molecules which show low-melting disordered mesophases[12] and rather exciting physical properties.[5b−d,13] Accordingly, for the aim of the present investigation, the "P-shaped" acetylacetonate complexes were chosen as more appropriate starting materials rather than the corresponding chloro-bridged dimers.

Oxidative addition reactions have been extensively performed on square-planar organoplatinum species, but within this field orthoplatinated complexes have been very seldom used.[14] Relatively few examples of Pt(IV) complexes prepared by the addition of X_2 or RX to Pt(II) precursors containing cyclometalated terdentate (NCN),[15] (NNC),[16] and (CNS)[17] or bidentate (CN) ligands[18,19] have been found in the literature. Therefore, the oxidative addition reaction on mononuclear cycloplatinated acetylacetonate complexes has to be tested.

The azobenzenes HL^{a-d} selected for this study are shown in Chart 1. In particular, the 4,4′-bis(methoxyazobenzene) ligand, HL^a, has been chosen as a reference compound to explore the synthetic procedures yielding cycloplatinated complexes, while the homologous HL^{b-d}

Chart 1. Stucture, Proton Numbering Scheme and Mesomorphism of the HL^{a-d} Ligands (K = Crystal; N = Nematic; Sm = Smectic, I = Isotropic)

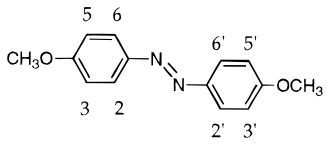

HL^a **K** 170 °C **I**

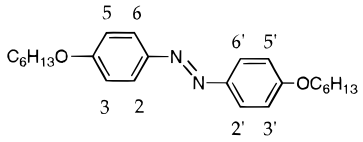

HL^b **K** 104 °C **N** 116 °C **I**

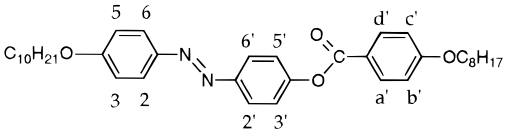

HL^c **K** 95 °C **SmC** 134 °C **N** 201 °C **I**

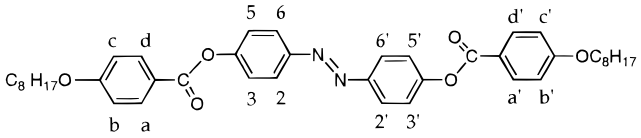

HL^d **K** 140 °C **SmC** 160 °C **N** 314 °C **I**

ligands are of interest in order to arrange a series of mesomorphic ligands (thermotropic behavior in Chart 1) bearing an increasing number of aromatic rings.[5d,8b]

Herein, the synthesis, characterization, and mesomorphic behavior of a series of dinuclear and mononuclear Pt(II) complexes, $[(L^{a-d})Pt(\mu\text{-}Cl)]_2$ and $[(L^{a-d})Pt(acac)]$, containing cyclometalated HL^{a-d} azobenzene ligands, are reported. Also described is the reactivity of the mononuclear Pt(II) derivatives $[(L^{a-d})Pt(acac)]$ with respect to the oxidative addition of iodine or methyl iodide, with formation of Pt(IV) cyclometalated species $[(L^{a-d})Pt(acac)I_2]$ and $[(L^{a-d})Pt(acac)(CH_3)I]$, respectively. Moreover, the X-ray crystal structure determinations of complexes $[(L^a)Pt(acac)]$, **2a**, $[(L^a)Pt(acac)I_2]$, **3a**, and $[(L^a)Pt(acac)(CH_3)I]$, **4a**, are presented.

The new complexes $[(L^{b-d})Pt(acac)I_2]$ and $[(L^{b-d})Pt(acac)(CH_3)I]$ show thermotropic mesomorphism. Remarkably, as far as we know, they are the first examples of Pt(IV) hexacoordinated liquid crystalline compounds.

Results and Discussion

Model Compounds. Synthesis and Characterization of the Cycloplatinated HL^a Compounds: Complexes 1a−4a. The synthetic procedures leading to the dinuclear Pt(II) and mononuclear Pt(II) or Pt(IV) complexes have been tested for the ligand 4,4′-bis(methoxyazobenzene), HL^a. The new compounds were characterized by elemental analyses, which accounted for the expected products and IR and ^1H NMR spectroscopies. The optimized synthetic procedures are summarized in Scheme 1.

(10) (a) Ryabov, A. D. *Chem. Rev.* **1990**, *90*, 403. (b) Ryabov, A. D. In *Perspectives In Coordination Chemistry*; Williams, A. F., Floriani, C., Merbach, A. E., Eds.; Verlag Helvetica Chimica Acta, Basel VCH: Weinheim, 1992; p 271.

(11) Pregosin, P. S.; Wombacher, F.; Albinati, A.; Lianza, F. *J. Organomet. Chem.* **1991**, *418*, 249.

(12) (a) Ghedini, M.; Pucci, D. *J. Organomet. Chem.* **1990**, *395*, 105. (b) Baena, M. J.; Espinet, P.; Ros, M. B.; Serrano, J. L. *Angew. Chem., Int. Ed. Engl.* **1991**, *30*, 711. (c) Ghedini, M.; Pucci, D.; Cesarotti, E.; Francescangeli, O.; Bartolino, R. *Liq. Cryst.* **1994**, *16*, 373.

(13) (a) Cipparrone, G.; Versace, C.; Duca, D.; Pucci, D.; Ghedini, M.; Umeton, C. *Mol. Cryst. Liq. Cryst.* **1992**, *212*, 217. (b) Scaramuzza, N.; Pagnotta, M. C. *Mol. Cryst. Liq. Cryst.* **1994**, *239*, 263.

(14) Rendina, L. M.; Puddephatt, R. J. *Chem. Rev.* **1997**, *97*, 1735.

(15) (a) van Koten, G.; Terheijden, J.; van Beek, J. A. M.; Wehman-Ooyevaar, I. C. M.; Muller, F.; Stam, C. H. *Organometallics* **1990**, *9*, 903. (b) Canty, A. J.; Honeyman, R. T. *J. Organomet. Chem.* **1990**, *387*, 247.

(16) (a) Anderson, C. M.; Crespo, M.; Jennings, M. C.; Lough, A. J.; Ferguson, G.; Puddephatt, R. J. *Organometallics* **1991**, *10*, 2672. (b) Anderson, C. M.; Crespo, M.; Ferguson, G.; Lough, A. J. G.; Puddephatt, R. J. *Organometallics* **1992**, *11*, 1177.

(17) Chattopadhyay, S.; Sinha, C.; Basu, P.; Chakravorty, A. *Organometallics* **1991**, *10*, 1135.

(18) Crespo, M.; Solans, X.; Font-Bardìa, M. *J. Organomet. Chem.* **1994**, *483*, 187.

(19) Chassot, L.; von Zelewsky, A.; Sandrini, D.; Maestri, M.; Balzani, V. *J. Am. Chem. Soc.* **1986**, *108*, 6084.

Scheme 1

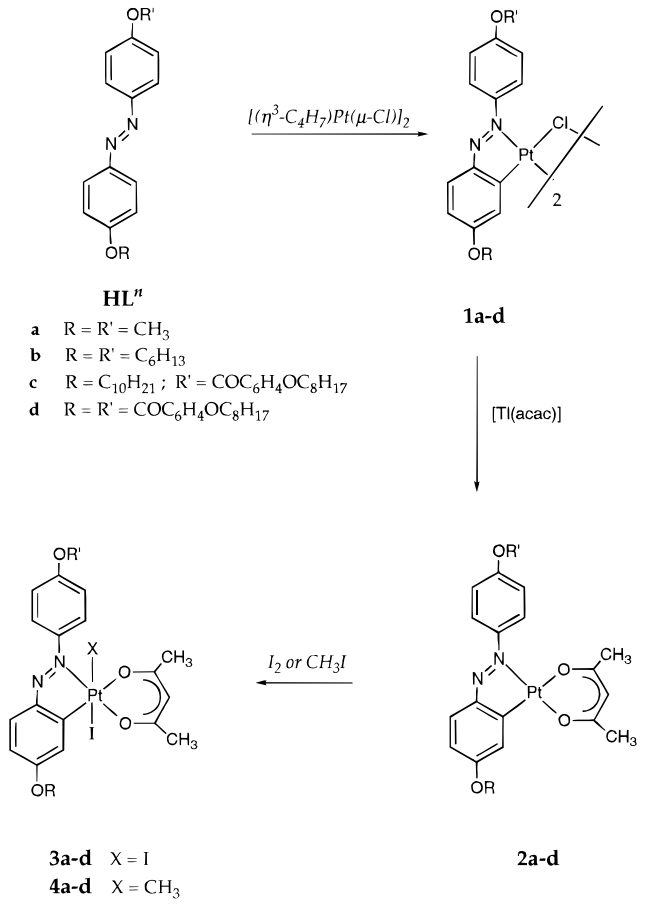

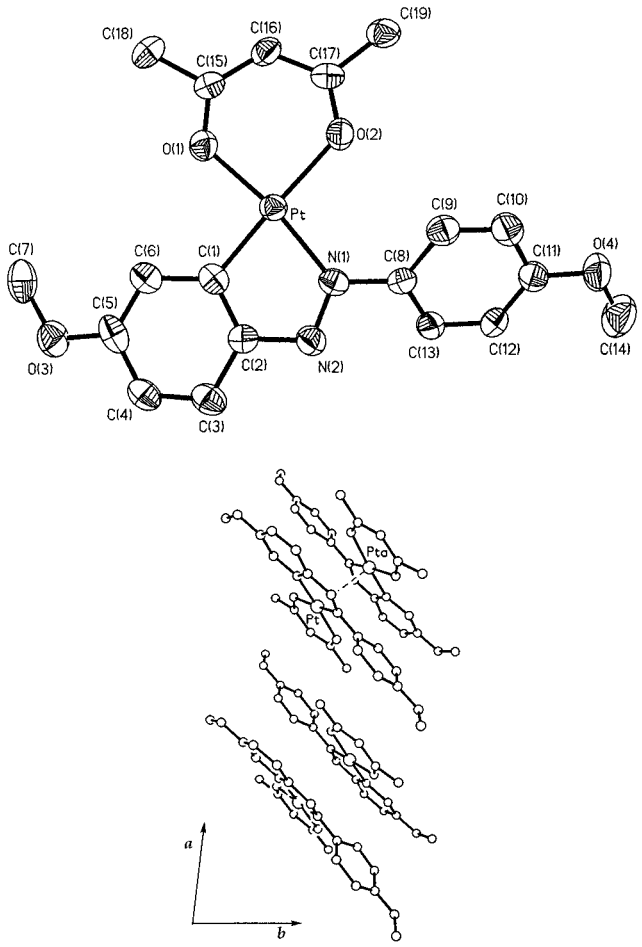

Figure 1. Molecular structure and atomic labeling scheme (40% probability thermal ellipsoids) (a); crystal packing down the *c* axis showing the shortest Pt- - -Pt intemolecular distance (b) of complex [(L^a)Pt(acac)], **2a**.

The cycloplatinated chloro-bridged dimer [(L^a)Pt(μ-Cl)]$_2$, **1a**, was prepared by treating HL^a with 2 equiv of [(η^3-C$_4$H$_7$)Pt(μ-Cl)]$_2$ in refluxing chloroform. The ^{1}H NMR spectrum (DMSO-d_6) of **1a** (Experimental Section) accounts for an orthometalated azobenzene since in the aromatic region signals attributable to two different phenyl rings are observed and the protons of the Pt(II)-bonded ring are significantly upfield shifted with reference to HL^a (for example, for the H(5) proton, $\Delta\delta$ = 0.92 ppm). Moreover, the proton ortho to the ligand-binding site, H(3), clearly shows a long-range coupling, of about 48 Hz, with the ^{195}Pt nuclei.

The mononuclear Pt(II) acetylacetonate derivative, [(L^a)Pt(acac)], **2a**, was obtained by reaction of **1a** with 2 equiv of [Tl(acac)], in dichloromethane solution, at room temperature. The ^{1}H NMR spectrum of **2a** is featured by the resonance at 5.50 ppm, assigned to the methinic proton of the acetylacetonate ligand. Comparison between the aromatic regions of the spectra of **1a** and **2a** shows two main differences, which confirm that the molecular structure changes from dinuclear to mononuclear: in **2a** a sizable deshielding effect is observed for all the aromatic protons (for example, for the H(5) proton, $\Delta\delta$ = 0.26 ppm) and the J_{Pt-H^3} decreases to about 39 Hz.

Reaction of **2a** with an equivalent amount of I_2 or a 10 molar excess of CH_3I, in acetone at room temperature, afforded the air-stable oxidative-addition platinum(IV) products [(L^a)Pt(acac)I$_2$], **3a** (dark violet), and [(L^a)Pt(acac)(CH$_3$)I], **4a** (brown-yellow), respectively. The ^{1}H NMR spectra of complexes **3a** and **4a**, compared to the spectra of the starting material **2a**, show a slight upfield shift of all the aromatic protons and a decreased value of $^3J_{Pt-H^3}$ (from 39 to 20, for **3a**, or to 25 Hz for **4a**). The $^3J_{Pt-H^3}$ data fall in the range characteristic for Pt(IV) species, confirming that oxidation of Pt(II) to Pt(IV) has actually occurred.[20]

Moreover, the ^{1}H NMR spectrum of **4a** shows a CH$_3$−Pt(IV) resonance, coupled to ^{195}Pt, at 1.22 ppm ($^2J_{Pt-H}$ = 65 Hz). Therefore, on the basis of this evidence, a trans oxidative addition of methyl iodide is proposed.[21] None of the compounds **1a**−**4a** show mesomorphic behavior, and all melt at temperatures that range from 180 °C (**4a**) to 298 °C (**1a**).

Crystal Structure Analysis of Complex [(L^a)Pt(acac)], 2a. The overall view of the molecule of **2a**, with the atom-labeling scheme, is shown in Figure 1a. Selected bond lengths and angles are listed in Table 1. Complex **2a** is essentially planar with the platinum atom in a distorted square-planar geometry. The maximum deviation is represented by the "bite" angle N(1)−Pt−C(1) of 79.0(3)°. This type of distortion is characteristic of cyclometalated Pt(II) complexes (80.7° is the mean N−Pt−C "bite" angle within the five-membered cycloplatinated ring of Pt(II) complexes reported in the literature). The bond distances and the other bond

(20) Monaghan, P. K.; Puddephatt, R. J. *Organometallics* **1985**, *4*, 1406.
(21) Clegg, D. E.; Hall, J. R.; Swile, G. A. *J. Organomet. Chem*. **1972**, *38*, 403.

Table 1. Selected Bond Distances (Å) and Angles (deg) for Complexes 2a−4a

	[(L^a)Pt(acac)], **2a**		
Pt−O(1)	1.985(6)	Pt−O(2)	2.078(6)
Pt−N(1)	1.991(6)	Pt−C(1)	1.947(9)
N(1)−N(2)	1.295(10)	N(2)−C(2)	1.405(9)
C(1)−C(2)	1.385(12)		
O(1)−Pt−O(2)	90.3(2)	O(1)−Pt−N(1)	170.2(3)
O(2)−Pt−N(1)	99.0(2)	O(1)−Pt−C(1)	91.5(3)
O(2)−Pt−C(1)	176.3(3)	N(1)−Pt−C(1)	79.0(3)
	[(L^a)Pt(acac)I$_2$], **3a**		
Pt−I(1)	2.654(1)	Pt−I(2)	2.644(1)
Pt−O(1)	2.004(6)	Pt−O(2)	2.133(6)
Pt−N(1)	2.021(6)	Pt−C(1)	1.975(8)
N(1)−N(2)	1.292(9)	N(2)−C(2)	1.370(12)
C(1)−C(2)	1.412(11)		
I(1)−Pt−I(2)	179.6(1)	I(1)−Pt−O(1)	88.1(2)
I(2)−Pt−O(1)	91.6(2)	I(1)−Pt−O(2)	90.1(2)
I(2)−Pt−O(2)	89.7(2)	O(1)−Pt−O(2)	91.1(2)
I(1)−Pt−N(1)	90.0(2)	I(2)−Pt−N(1)	90.3(2)
O(1)−Pt−N(1)	170.4(3)	O(2)−Pt−N(1)	98.3(3)
N(1)−Pt−C(1)	79.7(3)	I(1)−Pt−C(1)	90.8(3)
I(2)−Pt−C(1)	89.4(3)	O(1)−Pt−C(1)	90.9(3)
O(2)−Pt−C(1)	177.8(3)		
	[(L^a)Pt(acac)(CH$_3$)I], **4a**		
Pt−I(1)	2.744(3)	Pt−C(20)	2.181(19)
Pt−O(1)	2.009(15)	Pt−O(2)	2.156(15)
Pt−C(1)	1.986(24)	Pt−N(1)	2.047(19)
N(1)−N(2)	1.265(30)	N(2)−C(2)	1.386(31)
C(1)−C(2)	1.427(32)		
I(1)−Pt−N(1)	91.5(5)	I(1)−Pt−O(1)	90.9(6)
N(1)−Pt−O(1)	169.1(7)	I(1)−Pt−O(2)	91.7(5)
N(1)−Pt−O(2)	99.2(7)	O(1)−Pt−O(2)	91.3(6)
I(1)−Pt−C(1)	90.9(6)	N(1)−Pt−C(1)	79.6(8)
O(1)−Pt−C(1)	89.7(8)	O(2)−Pt−C(1)	177.1(8)
I(1)−Pt−C(20)	178.1(5)	N(1)−Pt−C(20)	90.2(7)
O(1)−Pt−C(20)	87.6(8)	O(2)−Pt−C(20)	87.1(7)
C(1)−Pt−C(20)	90.3(8)		

angles within the cycloplatinated ring are comparable with those found for the few structurally characterized platinum(II) complexes containing azobenzene ligands.[22] The coordination about the platinum atom is completed by two oxygen atoms of the *acac* ligand. The trans effect of the phenyl carbon C(1) bound to the Pt(II) center is marked by the longer Pt−O(2) bond length [2.078(6) Å], compared to the Pt−O(1) trans to the N(1) atom [1.985(6) Å]. This agrees with the trans influence of the coordinated carbon center generally observed in orthoplatinated complexes.[23] The bond distances and angles within the *acac* ligand are comparable with those found in other acetylacetonate Pt(II) complexes.[24] While the *acac* plane and the five-membered cycloplatinated ring are basically coplanar with a dihedral angle of 176.3(1)°, the rotationally free phenyl ring of the azobenzene ligand is twisted 32.0(8)° (average value) about the N−C bond with respect to the plane of the remainder of the complex.

In the crystal packing, compound **2a** forms dimeric units; the two molecules of the dimer are related to one another by a center of inversion (Figure 1b). The Pt- - -Pt distance of 3.311(1) Å implies some weak interaction between the two molecules, being in the range 3.76−3.15 Å observed in dimers of cyclometalated Pt(II) complexes.[25] Within the dimeric unit the two molecules are stacked along the *y* axis with an offset of 2.10 Å, and the distance between the five-membered cycloplatinated ring and the six-membered ring formed by the *acac* ligand is 3.40 Å.

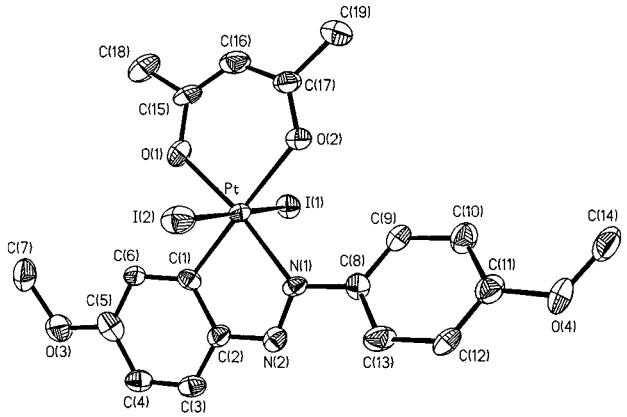

Figure 2. Molecular structure and atomic labeling scheme (40% probability thermal ellipsoids) of complex [(L^a)Pt(acac)I$_2$], **3a**.

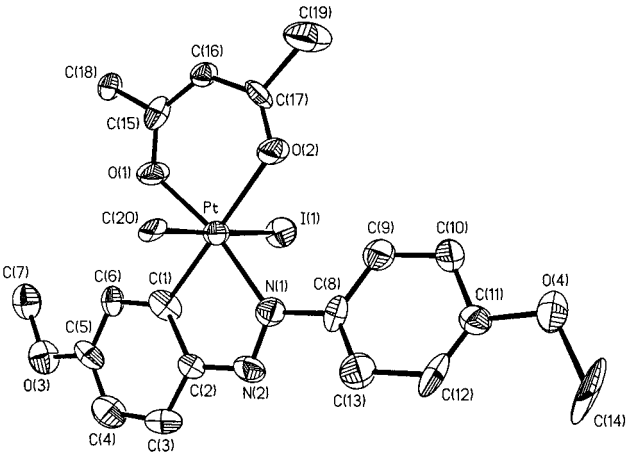

Figure 3. Molecular structure and atomic labeling scheme (40% probability thermal ellipsoids) of complex [(L^a)Pt(acac)(CH$_3$)I], **4a**.

Crystal Structure Analysis of Complexes [(L^a)Pt(acac)I$_2$], 3a, and [(L^a)Pt(acac)(CH$_3$)I], 4a. The crystal structures of **3a** and **4a**, with the pertinent atom-labeling schemes, are shown in Figures 2 and 3, respectively. Selected bond lengths and angles are listed in Table 1. The coordination geometry at the Pt atom is octahedral with the acetylacetonate and 4,4′-bis(methoxyazobenzene) ligands in the equatorial plane. The two iodine ligands in complex **3a** and the iodine and the methyl ligands in complex **4a** are trans to each other in the apical positions. Some distortion from regular geometry results from the small ′bite′ of the 4,4′-bis(methoxyazobenzene) as previously discussed for complex **2a** (Table 1). The Pt−I bond lengths of complex **3a** are comparable with those in other Pt(IV) complexes with trans iodide geometries,[26] while the sligthly larger value of 2.744(3) Å observed in complex **4a** reflects the

(22) (a) Elder, R. C.; Cruea, R. D. P.; Morrison, R. F. *Inorg. Chem.* **1976**, *15*, 1623. (b) Chattopadhyay, S.; Sinha, C.; Basu, P.; Chakravorty, A. *J. Organomet. Chem.* **1991**, *414*, 421.

(23) Mdleleni, M. M.; Bridgewater, J. S.; Watts, R. J.; Ford, P. C. *Inorg. Chem.* **1995**, *34*, 2334.

(24) Katoh, H.; Miki, K.; Kai, Y.; Tanaka, N.; Kasai, N. *Bull. Chem. Soc. Jpn.* **1981**, *54*, 611.

(25) (a) Breu, J.; Range, K.-J.; von Zelewsky, A.; Yersin, H. *Acta Crystallogr.* **1997**, *C53*, 562. (b) Bandyopadhyay, D.; Bandyopadhyay, L.; Chakravorty, A.; Cotton, F.; Falvello, L. R. *Inorg. Chem.* **1983**, *22*, 1315.

trans influence of the methyl ligand.[27] The bond distances and angles within the five-membered cycloplatinated ring and the *acac* ligand in both complexes **3a** and **4a** are similar to those found in complex **2a**.

Mesogenic Compounds. Synthesis and Characterization of the Cycloplatinated HL^{b-d} Compounds: Complexes 1b−d to 4b−d. The synthetic procedures tested for HL^{a} have been extended to the series HL^{b-d} (Chart 1) to obtain Pt(IV) complexes with liquid crystalline properties. The 4,4′-disubstituted azobenzenes HL^{b-d} were prepared as previously reported, while their cycloplatinated complexes **1b−d** to **4b−d** were synthesized as described for complexes **1a−4a** (Scheme 1).

All compounds, purified by recrystallization from suitable solvents (Experimental Section), are air-stable solids which give satisfactory elemental analyses and were characterized by IR and ^{1}H NMR spectroscopies.

The dinuclear chloro-bridged [(L^{b-d})Pt(μ-Cl)]$_2$ complexes **1b−d** display an ^{1}H NMR spectral pattern analogous to that of **1a**, with the H(3) and H(5) protons shielded about 0.2 and 0.3 ppm, respectively, with reference to the parent uncomplexed ligands. Moreover, the ^{1}H NMR spectrum of **1c** shows that the reaction product is a 9:1 mixture of the two isomers, **1c(A)** and **1c(B)**, which form by a nonselective platination of the 4,4′-asymmetrically substituted azobenzene HL^{c}. Comparison of the ^{1}H NMR spectra of **1c** and **1d** allows us to conclude that the major isomer is **1c(A)**. Thus in HL^{c} metalation preferably occurs at the more electron-rich phenyl ring.

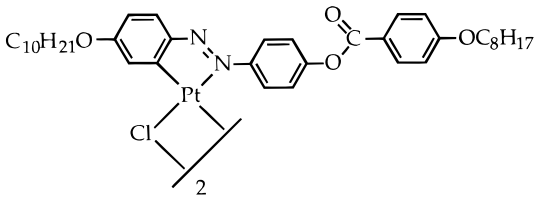

1c(A)

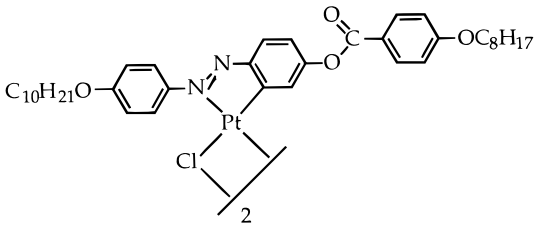

1c(B)

The mononuclear square-planar β-diketonate compounds, [(L^{b-d})Pt(acac)], **2b−d** give very similar ^{1}H NMR spectra and show a $^3J_{Pt-H^3}$ of about 36 Hz.

Complexes **2b** and **2c** react with a stoichiometric amount of iodine or methyl iodide to give rise to [(L^{b-d})Pt(acac)I$_2$] and [(L^{b-d})Pt(acac)(CH$_3$)I] derivatives, **3b,c** and **4b,c**, respectively. In similar reactions a large excess of iodine (molar ratio 1:3) or methyl iodide (molar ratio 1:100) was necessary to obtain **3d** and **4d** (Experimental Section). The ^{1}H NMR spectra of **2c**, **3c**, and **4c** account for a pure compound arising from the more abundant isomer **1c(A)**. Moreover, in series **3** and **4**, the values of both the coupling constants $^3J_{Pt-H^3}$ and $^2J_{Pt-H}$ fall in the same range detected for **3a** and **4a**; thus all the obtained results agree well with the general formula sketched in Scheme 1.

Table 2. Optical and Thermal Properties of the Square-Planar Pt(II) [(L^{b-d})Pt(μ-Cl)]$_2$, 1b−d, and [(L^{b-d})Pt(acac)], 2b−d, Complexes

compound	transition[a]	T/°C	ΔH/kJ mol^{-1} [b]
1b	K−I	232[c]	
1c	K−SmC	206	26.0
	SmC−N	253	2.9
	N−I	275[d]	
1d	K−SmC	263	37.1
	SmC−I	342[c,d]	
2b	K−I	129	44.4
	I−N	109	1.0
	N−K	87	33.3
2c	K−K′	124	34.2
	K′−N	131	1.4
	N−I	196	1.4
	I−N	202[c]	
	N−K	89	27.4
2d	K−N	185	36.2
	N−I	250[c,d]	

[a] K = crystal, N = nematic, Sm = smectic, I = isotropic. [b] Data from DSC for second heating cycle. [c] Data from optical observations. [d] Decomposition.

Table 3. Optical and Thermal Properties of the Octahedral Pt(IV) [(L^{b-d})Pt(acac)I$_2$], 3b−d, and [(L^{b-d})Pt(acac)(CH$_3$)I], 4b−d, Complexes

compound	transition[a]	T/°C	ΔH/kJ mol^{-1} [b]
3b	K−I	149[c]	
3c	K−I	125	30.7
	I−E	60	0.5
3d	K−N	178	50.0
	N−I	180	0.7
4b	K−I	134	38.9
4c	K−N	108	21.2
	N−I	230[c,d]	
4d	K−SmC	110[c]	
	SmC−N	142	64.9
	N−I	270[d]	

[a] K = crystal, E = crystal, N = nematic, Sm = smectic, I = isotropic. [b] Data from DSC for second heating cycle. [c] Data from optical observations. [d] Decomposition.

Mesogenic Behavior of Complexes 1b−d to 4b−d. The mesophases were first identified according to their textures[28] observed by polarized optical microscopy and then investigated by differential scanning calorimetry. All the HL^{b-d} are mesomorphic and exhibit an enantiotropic nematic phase (N) which, in the case of HL^{c} and HL^{d}, appears before the smectic C (SmC) (Chart 1).

Tables 2 and 3 summarize the transition temperatures, enthalpies, and types of mesophases observed for the platinum complexes that the HL^{b-d} ligands form.

The binuclear complex **1b**, derived from 4,4′-bis(hexyloxyazobenzene) HL^{b}, loses the liquid crystalline behavior displayed by its organic precursor and, on heating, directly melts (232 °C) to the isotropic liquid

(26) (a) van Beek, J. A. M.; van Koten, G.; Wehman-Ooyevaar, I. C. M.; Smeets, W. J. J.; van der Sluis, P.; Spek, A. L. *J. Chem. Soc., Dalton Trans.* **1991**, 883. (b) Cheetham, A. K.; Puddephatt, R. J.; Zalkin, A.; Templeton, D. H.; Templeton, L. K. *Inorg. Chem.* **1976**, *15*, 2997. (c) Cook, P. M.; Dahl, L. F.; Hopgood, D.; Jenkins, R. A. *J. Chem. Soc., Dalton Trans.* **1973**, 294.

(27) Albano, V. G.; Braga, D.; De Felice, V.; Panunzi, A.; Vitagliano, A. *Organometallics* **1987**, *6*, 517.

(28) (a) Demus, D.; Richter, L. *Textures of Liquid Crystals*; Verlag Chemie: Weinheim−New York, 1978. (b) Gray, G. W.; Goodby, J. W. *Smectic Crystal Textures and Structures*; Leonard Hill: Glasgow, 1984.

(I). Complex **1c**, however, shows an SmC phase at 206 °C, with the typical schlieren texture, before giving way to a N phase at 253 °C. Finally, complex **1d** displays only a SmC phase (exhibiting a schlieren texture), which appears at 262 °C. For both **1c** and **1d** the transition from liquid crystal to I (275 and 342 °C, respectively) is accompanied by strong decomposition. With reference to their parent ligands, a stabilization of the more ordered SmC phase is observed for both **1c** and **1d**, while as the thermal properties are concerned, the melting temperatures increase more than the clearing ones, so that the mesomorphic range decreases.

On going from the binuclear **1b**−**d** to the mononuclear **2b**−**d** Pt(II) complexes, it is evident (Table 2) that the change in the molecular structure from "H-shaped" to "P-shaped" (Scheme 1) promotes the mesomorphism. A restoration of liquid crystallinity, which consists of a monotropic N phase, stable from 109 to 87 °C, is indeed observed for **2b**. Moreover, for **2c** and **2d**, the enantiotropic SmC phase observed in the dimeric parents becomes N (schlieren textures; range of stability: **2c**, 131−196 °C; **2d**: 185−250 °C), and the transition to the I phase takes place with extensive decomposition. In both compounds, by reducing the symmetry of the molecules, the melting and the clearing points are brought down in temperature, and for the **2d** complex, a broadening of the mesomorphism is achieved. It is worth noting that species **2b**−**d** show a less ordered mesophase and clearing temperatures lower even than those of the corresponding HL^{b-d} ligands.

Liquid crystalline properties dramatically change by oxidative addition of I_2 and CH_3I to acetylacetonate Pt(II) substrates. To promote mesomorphic behavior in octahedral complexes,[8a] organic ligands of increasing molecular length, fairly anisotropic in shape to compensate for the structural perturbation induced by the six-coordinate platinum center, were selected. Thus the 4,4′-bis(hexyloxyazobenzene) derivative **3b**, which does not have the appropriate molecular anisotropy to balance the introduction of two ligands in axial positions, loses its mesomorphism and the microcrystalline solid melts directly to an isotropic liquid at 149 °C. Upon cooling from the I phase, **3b** did not crystallize, but froze in a glassy state which is stable over months. The presence of a further aromatic ring in the mesogenic ligand of compound **3c** led to destabilization of the mesomorphism of the square-planar Pt(II) parent complex, transforming the enantiotropic N into the monotropic E mesophase (mosaic texture). In addition, on cooling, complex **3c** retains the E ordering, giving a glassy solid, stable for a long time. Interestingly, when the azobenzene core of these hexacoordinated complexes is symmetrically added onto by two benzoate groups, the Pt(IV) diodio derivative, **3d**, preserves the same mesomorphic behavior of **2d** and exhibits an enantiotropic N phase between 177 and 180 °C. The clearing points of **3c** and **3d** are lower by about 70 °C than those of **2c** and **2d**, and no decomposition was observed.

The $[(L^{b-d})Pt(acac)(CH_3)I]$ compounds **4c** and **4d** retain the mesophase which is shown by **2c** and **2d**, while **4b** is not mesogenic at all. In particular, **4c** forms, at 108 °C, an enantiotropic N phase, exhibiting a marbled texture, which is stable until 230 °C, and **4d** shows an SmC phase (at 110 °C), followed by the N one which occurs between 142 and 270 °C. As a general trend, it should be pointed out that substitution of I_2 for CH_3I in the oxidative addition to $[(L^{c-d})Pt(acac)]$ complexes causes a large reduction in the melting points. Contrarily, the corresponding clearing temperatures increase and a strong decomposition takes place when the I phase forms. It is worth noting that both **4c** and **4d** exhibit mesomorphism over a temperature range (122 and 160 °C, respectively) that is much wider than the corresponding square-planar homologous **2c** and **2d** (65 °C). Furthermore, as confirmed by calorimetric and ^1H NMR measurements carried out on melted samples or after annealing experiments performed in the mesophase some degrees before the clearing temperature, on heating, compounds **4b**−**d** quantitatively revert to the respective Pt(II) starting materials **2b**−**d**. Thus, the oxidative addition of methyl iodide to $[(L^{b-d})Pt(acac)]$ complexes is a reversible process.

Conclusions

The HL^{a-d} azobenzene ligands undergo orthometalation by reaction with $[(\eta^3\text{-}C_4H_7)Pt(\mu\text{-}Cl)]_2$ in mild conditions. The ligand HL^c, asymmetrically substituted (Chart 1), preferentially underwent cyclometalation at the most electron-rich azo-bonded aromatic ring. Thus the orthoplatination of azobenzenes can be considered electrophilic in character.[29]

The dinuclear species give rise to the corresponding mononuclear derivatives $[(L^{a-d})Pt(acac)]$. The molecular structure of complex $[(L^a)Pt(acac)]$, **2a**, has been determined by single-crystal X-ray analysis, and the shortest intermolecular Pt- - -Pt distance of 3.311(1) Å has been found between two molecules related by a center of inversion which form dimeric units in the crystal packing.

The mononuclear Pt(II) complexes undergo oxidative addition reaction with I_2 or CH_3I. The trans-addition has been confirmed by the X-ray crystal structure analysis performed on the model compounds $[(L^a)Pt(acac)I_2]$, **3a**, and $[(L^a)Pt(acac)(CH_3)I]$, **4a**.

The addition of two ligands changes the coordination geometry of the metal atom from square-planar to octahedral so that, in the solid state, intermolecular nonbonding Pt- - -Pt interactions are not observed. These interactions may also be at work in the mesophases, and their disappearance should account for the sizable lowering of the clearing temperatures the Pt(IV) mesogens show with reference to the respective Pt(II) parent complexes. Moreover, comparing the I_2 with the CH_3I addition products, it should be pointed out that, replacing an iodine atom with the bulkier methyl group, the melting points decrease whereas the clearing temperatures increase. Hence, by substitution of a CH_3 group with an I atom, the mesophases become stable over a wider temperature range.

The oxidative addition of CH_3I to the $[(L^{b-d})Pt(acac)]$ compounds is a process that can be made reversible on heating. Both the starting Pt(II) and the final Pt(IV) complexes are liquid crystals; interestingly, this outcome could be of interest for the development of syntheses in an oriented reaction media.

Concluding, we succeded in the preparation of octahedral Pt(IV) mesogens by oxidative addition to Pt(II)

(29) Cope, A. C.; Siekman, R. W. *J. Am. Chem. Soc.* **1965**, *87*, 3272.

acetylacetonate complexes. This synthetic procedure can be extended to addenda other than I_2 or CH_3I, and in principle, a wide family of differently functionalized liquid crystalline Pt(IV), tailored for specific physical properties, could become available.

Experimental Section

General Comments. All the commercially available chemicals were used as received. $[K_2(PtCl_4)]$ was purchased from Johnson-Matthey Inc. Literature methods were used to prepare $[(\eta^3\text{-}C_4H_7)Pt(\mu\text{-}Cl)]_2$[30] and [Tl(acac)].[31] The HL^b, HL^c, and HL^d ligands were synthesized as previously reported (refs 32, 8b, and 5d, respectively). The infrared spectra were recorded on a Perkin-Elmer FT 2000, as KBr pellets. The ^1H NMR spectra were recorded on a Bruker WH-300 spectrometer in $CDCl_3$ or $(CD_3)_2SO$ solutions, with TMS as internal standard. Elemental analyses were performed with a Perkin-Elmer 2400 analyzer. Optical observations were made with a Zeiss Axioscope polarizing microscope equipped with a Linkam C0 600 heating stage. The transition temperatures and enthalpies were measured on a Perkin-Elmer DSC-7 differential scanning calorimeter with a heating and cooling rate of 10 °C/min. The apparatus was calibrated with indium (156.6 °C, 3.3 kJ mol^{-1}) and tin (232.1 °C, 7.2 kJ mol^{-1}). Two or more heating/cooling cycles were performed on each sample.

Preparation of $[(L^{a-d})Pt(\mu\text{-}Cl)]_2$ Complexes. The preparation of compound $[(L^a)Pt(\mu\text{-}Cl)]_2$, **1a**, is described in detail; all other homologues were prepared similarly.

$[(L^a)Pt(\mu\text{-}Cl)]_2$, 1a. HL^a ligand (121 mg, 0.50 mmol) was added to a solution of $[(\eta^3\text{-}C_4H_7)Pt(\mu\text{-}Cl)]_2$ (143 mg, 0.25 mmol) in chloroform (15 mL). The mixture was heated at reflux for 35 h, cooled to room temperature, and filtered off; the dark-red solid was crystallized from chloroform, filtered, and dried under vacuum to give the pure product in 76% yield (180 mg). Mp: 298 °C. Anal. Calcd for $C_{28}Cl_2H_{26}N_4O_4Pt_2$: C, 35.64; H, 2.78; N, 5.94. Found: C, 34.71; H, 2.66; N, 5.83. ^1H NMR ($(CD_3)_2SO$): δ (ppm) 7.13 (d, $J = 8.5$ Hz, 1H; H^6), 6.90 (d, $J = 1.9$ Hz, 1H; H^3), 6.72 (d, $J = 8.65$ Hz, 2H; $H^{2',6'}$), 6.15 (d, $J = 8.65$ Hz, 2H; $H^{3',5'}$), 6.08 (dd, $J = 8.5, 1.9$ Hz, 1H; H^5), 3.02 (s, 3H; OCH_3), 2.98 (s, 3H; OCH_3), $^3J(^{195}Pt-H_3) = 48$ Hz.

Colors, solvent, reaction times, yields, melting points, and analytical and ^1H NMR data for complexes **1b**−**d** are as follows.

$[(L^b)Pt(\mu\text{-}Cl)]_2$, 1b: red; chloroform; 26 h; yield 166 mg (72%); mp 232 °C. Anal. Calcd for $C_{48}Cl_2H_{66}N_4O_4Pt_2$: C, 47.10; H, 5.43; N, 4.58. Found: C, 47.50; H, 5.40; N, 4.47.

$[(L^c)Pt(\mu\text{-}Cl)]_2$, 1c: red; toluene; 18 h; yield 89 mg (62%); thermotropic behavior in Table 2. Anal. Calcd for $C_{74}Cl_2H_{98}N_4O_8Pt_2$: C, 54.44; H, 6.05; N, 3.43. Found: C, 54.55; H, 6.04; N, 3.30. ^1H NMR ($CDCl_3$), isomer A: δ (ppm) 8.15 (d, $J = 8.8$ Hz, 2H; $H^{a',d'}$), 7.81 (d, $J = 8.8$ Hz, 2H; $H^{2',6'}$), 7.80 (d, $J = 8.7$ Hz, 1H; H^6), 7.35 (d, $J = 8.8$ Hz, 2H; $H^{3',5'}$), 6.98 (d, $J = 8.8$ Hz, 2H; $H^{b',c'}$), 6.78 (d, 1H; H^3), 6.71 (dd, 1H; H^5), 4.05 (m, 4H; OCH_2).

$[(L^d)Pt(\mu\text{-}Cl)]_2$, 1d: red; toluene; 16 h; yield 175 mg (65%); thermotropic behavior in Table 2. Anal. Calcd for $C_{84}Cl_2H_{98}N_4O_{12}Pt_2$: C, 55.53; H, 5.44; N, 3.08. Found: C, 55.97; H, 5.51; N, 2.70. ^1H NMR ($CDCl_3$): δ (ppm) 8.10 (d, $J = 9.1$ Hz, 2H; $H^{a',d'}$), 8.07 (d, $J = 9.1$ Hz, 2H; $H^{a,d}$), 7.96 (d, $J = 8.4$ Hz, 1H; H^6), 7.86 (d, $J = 8.8$ Hz, 2H; $H^{2',6'}$), 7.39 (d, $J = 8.8$ Hz, 2H; $H^{3',5'}$), 7.13 (d, $J = 2.0$ Hz, 1H; H^3), 7.09 (dd, $J = 8.4$, 2.0 Hz, 1H; H^5), 6.94 (d, $J = 9.1$ Hz, 2H; $H^{b',c'}$), 6.89 (d, $J = 9.1$ Hz, 2H; $H^{b,c}$), 4.04 (t, 2H; OCH_2), 4.00 (t, 2H; OCH_2).

Preparation of $[(L^{a-d})Pt(acac)]$ Complexes. The preparation of compound $[(L^a)Pt(acac)]$, **2a**, is described in detail; all other homologues were prepared similarly.

$[(L^a)Pt(acac)]$, 2a. A mixture of **1a** (113 mg, 0.12 mmol) and [Tl(acac)] (73 mg, 0.24 mmol) in dichloromethane (15 mL) was stirred at room temperature for 6 h. The reaction mixture was filtered off and the solution evaporated under reduced pressure. The solid was crystallized from methanol, filtered, and dried under vacuum. A brown solid was obtained in 83% yield (104 mg). Mp: 200 °C. Anal. Calcd for $C_{19}H_{20}N_2O_4Pt$: C, 42.62; H, 3.76; N, 5.23. Found: C, 42.32; H, 3.72; N, 4.66. ^1H NMR ($CDCl_3$): δ (ppm) 7.89 (d, $J = 9.1$ Hz, 2H; $H^{2',6'}$), 7.88 (d, $J = 8.6$ Hz, 1H; H^6), 7.09 (d, $J = 2.8$ Hz, 1H; H^3), 6.96 (d, $J = 9.1$ Hz, 2H; $H^{3',5'}$), 6.74 (dd, $J = 8.6, 2.8$ Hz, 1H; H^5), 5.50 (s, 1H; $CH{=}C(CH_3)_2$), 3.94 (s, 3H; OCH_3), 3.88 (s, 3H; OCH_3), 2.06 (s, 3H; CH_3CO), 1.97 (s, 3H; CH_3CO); $^3J(^{195}Pt-H_3) = 39$ Hz.

Colors, reaction times, yields, melting points, and analytical and ^1H NMR data for complexes **2b**−**d** are as follows.

$[(L^b)Pt(acac)]$, 2b: red; 4.5 h; yield 97 mg (92%); thermotropic behavior in Table 2. Anal. Calcd for $C_{29}H_{40}N_2O_4Pt$: C, 51.55; H, 5.97; N, 4.15. Found: C, 51.07; H, 6.01; N, 4.19. ^1H NMR ($CDCl_3$): δ (ppm) 7.87 (d, $J = 9.0$ Hz, 2H; $H^{2',6'}$), 7.86 (d, $J = 8.6$ Hz, 1H; H^6), 7.06 (d, $J = 2.5$ Hz, 1H; H^3), 6.94 (d, $J = 9.0$ Hz, 2H; $H^{3',5'}$), 6.72 (dd, $J = 8.6, 2.5$ Hz, 1H; H^5), 5.50 (s, 1H; $CH{=}C(CH_3)_2$), 4.12 (t, 2H; OCH_2), 4.02 (t, 4H; OCH_2), 2.06 (s, 3H; CH_3CO), 1.97 (s, 3H; CH_3CO); $^3J(^{195}Pt-H_3) = 36$ Hz.

$[(L^c)Pt(acac)]$, 2c: red; 2.5 h; yield 73 mg (92%); thermotropic behavior in Table 2. Anal. Calcd for $C_{42}H_{56}N_2O_6Pt$: C, 57.32; H, 6.41; N, 3.18. Found: C, 57.29; H, 6.41; N, 3.59. ^1H NMR ($CDCl_3$): δ (ppm) 8.17 (d, $J = 8.8$ Hz, 2H; $H^{a',d'}$), 7.98 (d, $J = 8.9$ Hz, 2H; $H^{2',6'}$), 7.91 (d, $J = 8.7$ Hz, 1H; H^6), 7.32 (d, $J = 8.9$ Hz, 2H; $H^{3',5'}$), 7.09 (d, $J = 2.5$ Hz, 1H; H^3), 6.99 (d, $J = 8.8$ Hz, 2H; $H^{b',c'}$), 6.75 (dd, $J = 8.7, 2.5$ Hz, 1H; H^5), 5.51 (s, 1H; $CH{=}C(CH_3)_2$), 4.14 (t, 2H; OCH_2), 4.05 (t, 2H; OCH_2), 2.08 (s, 3H; CH_3CO), 1.99 (s, 3H; CH_3CO).

$[(L^d)Pt(acac)]$, 2d: dark-red; 6 h; yield 114 mg (89%); thermotropic behavior in Table 2. Anal. Calcd for $C_{47}H_{56}N_2O_8Pt$: C, 58.07; H, 5.81; N, 2.88. Found: C, 57.92; H, 5.70; N, 2.83. ^1H NMR ($CDCl_3$): δ (ppm) 8.19 (d, $J = 8.7$ Hz, 2H; $H^{a',d'}$), 8.17 (d, $J = 8.7$ Hz, 2H; $H^{a,d}$), 8.08 (d, $J = 8.5$ Hz, 1H; H^6), 8.03 (d, $J = 8.9$ Hz, 2H; $H^{2',6'}$), 7.42 (d, $J = 2.3$ Hz, 1H; H^3), 7.36 (d, $J = 8.9$ Hz, 2H; $H^{3',5'}$), 7.09 (dd, $J = 8.5, 2.3$ Hz, 1H; H^5), 6.99 (d, $J = 8.7$ Hz, 4H; $H^{b,c,b',c'}$), 5.50 (s, 1H; $CH{=}C(CH_3)_2$), 4.05 (t, 4H; OCH_2), 2.06 (s, 3H; CH_3CO), 1.99 (s, 3H; CH_3CO); $^3J(^{195}Pt-H_3) = 32$ Hz.

Preparation of $[(L^{a-d})Pt(acac)I_2]$ Complexes. The preparation of compound $[(L^a)Pt(acac)I_2]$, **3a**, is described in detail; all other homologues were prepared similarly.

$[(L^a)Pt(acac)I_2]$, 3a. A solution of 33 mg of I_2 (0.13 mmol) in acetone (3 mL) was added to a suspension of **2a** (72 mg, 0.13 mmol) in acetone (6 mL). The solution immediately turned yellow and was allowed to stir, at room temperature, for 75 min. The solvent volume was reduced, and a dark-violet solid was filtered off and dried under vacuum to give the pure product in 90% yield (96 mg). Mp: 246 °C. Anal. Calcd for $C_{19}H_{20}I_2N_2O_4Pt$: C, 28.91; H, 2.55; N, 3.55. Found: C, 28.86; H, 2.56; N, 3.00. ^1H NMR ($CDCl_3$): δ (ppm) 8.13 (d, $J = 8.5$ Hz, 1H; H^6), 8.04 (d, $J = 8.6$ Hz, 2H; $H^{2',6'}$), 7.02 (d, $J = 2.5$ Hz, 1H; H^3), 7.00 (d, $J = 8.6$ Hz, 2H; $H^{3',5'}$), 6.87 (dd, $J = 8.5$, 2.5 Hz, 1H; H^5), 5.60 (s, 1H; $CH{=}C(CH_3)_2$), 4.03 (s, 3H; OCH_3), 3.92 (s, 3H; OCH_3), 2.17 (s, 3H; CH_3CO), 2.15 (s, 3H; CH_3CO); $^3J(^{195}Pt-H_3) = 20$ Hz.

Colors, reaction times, yields, melting points, and analytical and ^1H NMR data for complexes **3b**−**d** are as follows.

$[(L^b)Pt(acac)I_2]$, 3b: red; 75 min; crystallization from methanol; yield 62 mg (90%); mp 149 °C. Anal. Calcd for $C_{29}H_{40}I_2N_2O_4Pt$: C, 37.47; H, 4.34; N, 3.01. Found: C, 37.99; H, 4.37; N, 3.07. ^1H NMR ($CDCl_3$): δ (ppm) 8.10 (d, $J = 8.9$ Hz, 1H; H^6), 8.01 (d, $J = 9.1$ Hz, 2H; $H^{2',6'}$), 6.99 (d, $J = 2.5$ Hz, 1H; H^3), 6.97 (d, $J = 9.1$ Hz, 2H; $H^{3',5'}$), 6.84 (dd, $J = 8.9$, 2.5 Hz, 1H; H^5), 5.59 (s, 1H; $CH{=}C(CH_3)_2$), 4.20 (t, 2H; OCH_2), 4.05 (t, 2H; OCH_2), 2.17 (s, 3H; CH_3CO), 2.14 (s, 3H; CH_3CO); $^3J(^{195}Pt-H_3) = 20$ Hz.

(30) Mabbot, D. J.; Mann, B. E.; Maitlis, P. M. *J. Chem. Soc., Dalton Trans.* **1977**, 294.

(31) Taylor, E. C.; Hawks, G. H.; Mckillop, A. *J. Am. Chem. Soc.* **1968**, *90*, 2421.

Table 4. Crystallographic Data for Complexes 2a−4a

	[(L^a)Pt(acac)], **2a**	[(L^a)Pt(acac)I$_2$], **3a**	[(L^a)Pt(acac)(CH$_3$)I], **4a**
empirical formula	$C_{19}H_{21}N_2O_4Pt$	$C_{19}H_{21}I_2N_2O_4Pt$	$C_{20}H_{24}IN_2O_4Pt$
fw	536.5	790.3	678.4
cryst syst	triclinic	triclinic	orthorombic
space group	$P\bar{1}$	$P\bar{1}$	$P2_12_12_1$
a, Å	9.390(3)	7.687(3)	10.335(3)
b, Å	9.830(4)	10.155(3)	13.015(9)
c, Å	10.366(3)	15.604(6)	16.386(4)
α, deg	96.62(3)	95.59(3)	90
β, deg	100.08(2)	94.08(3)	90
γ, deg	94.62(3)	109.75(2)	90
V, Å^3	930.7(5)	1133.9(7)	2204(2)
Z	2	2	4
F(000)	518	730	1284
ρ(calc.), g/cm^3	1.914	2.315	2.044
μ, cm^{-1}	75.64	39.36	77.94
transmission factors	0.068/0.103	0.271/0.898	0.030/0.073
T, °C	25	25	25
λ, Å	0.710 73	0.710 73	0.710 73
2θ range for data collection	3.5−50.0	3.5−50.0	3.5−50.0
no. of reflns collected	3558	4305	2229
no. of ind reflns	3250 [R(int) = 0.0502]	3979 [R(int) = 0.0486]	2209 [R(int) = 0.000]
no. of data/restraints/params	3003/0/235	3202/0/253	2077/0/253
R^a [$I > 2\sigma(I)$]	0.032	0.043	0.064
R^{1b}	0.040	0.047	0.071
goodness-of-fit	0.50	1.39	1.85

^{a} $R = \Sigma||F_o| - |F_c||/\Sigma|F_o|$. ^{b} $R^1 = [\Sigma w(|F_o| - |F_c|)^2/\Sigma w|F_o|^2]^{1/2}$.

[(L^c)Pt(acac)I$_2$], 3c: red; 1 h; crystallization from methanol; yield 47 mg (89%); thermotropic behavior in Table 3. Anal. Calcd for $C_{42}H_{56}I_2N_2O_6Pt$: C, 44.49; H, 4.98; N, 2.47. Found: C, 44.77; H, 5.01; N, 2.81. ^{1}H NMR ($CDCl_3$): δ (ppm) 8.18−8.10 (m, 5H; H$^{a',d',2',6',6}$), 7.37 (d, J = 8.9 Hz, 2H; H$^{3',5'}$), 7.02−6.98 (m, 3H; H$^{3,b',c'}$), 6.87 (dd, J = 8.8, 2.2 Hz, 1H; H^5), 5.60 (s, 1H; CH=C(CH$_3$)$_2$), 4.22 (t, 2H; OCH$_2$), 4.05 (t, 2H; OCH$_2$), 2.18 (s, 3H; CH$_3$CO), 2.15 (s, 3H; CH$_3$CO).

[(L^d)Pt(acac)I$_2$], 3d: 3 equiv of I_2; dark-red; 30 min; yield 24 mg (60%); thermotropic behavior in Table 3. Anal. Calcd for $C_{47}H_{56}I_2N_2O_8Pt$: C, 46.05; H, 4.60; N, 2.28. Found: C, 45.65; H, 4.50; N, 2.35. ^{1}H NMR ($CDCl_3$): δ (ppm) 8.35 (d, J = 8.6 Hz, 1H; H^6), 8.19 (d, J = 8.9 Hz, 2H; H$^{2',6'}$), 8.18 (dd, J = 8.9 Hz, 2H; H$^{a,d,a',d'}$), 7.45 (d, J = 2.3 Hz, 1H; H^3), 7.42 (d, J = 8.9 Hz, 2H; H$^{3',5'}$), 7.34 (dd, J = 8.6, 2.3 Hz, 1H; H^5), 7.01 (d, J = 8.9 Hz, 2H; H$^{b',c'}$), 7.00 (d, J = 8.9 Hz, 2H; H^{b,c}), 5.63 (s, 1H; CH=C(CH$_3$)$_2$), 4.07 (t, 4H; OCH$_2$), 2.19 (s, 3H; CH$_3$CO), 2.17 (s, 3H; CH$_3$CO); $^3J(^{195}Pt-H_3)$ = 18 Hz.

Preparation of [(L^{a-d})Pt(acac)(CH$_3$)I] Complexes. The preparation of compound [(L^a)Pt(acac)(CH)$_3$I], **4a**, is described in detail; all other homologues were prepared similarly.

[(L^a)Pt(acac)(CH$_3$)I], 4a. CH$_3$I (1.71 mmol) was added to a suspension of **2a** (90 mg, 0.17 mmol) in acetone (10 mL) and stirred for 4 days. Concentration of the resulting yellow solution followed by addition of diethyl ether resulted in the formation of a brownish solid, which was filtered off and dried under vacuum. Yield: 91 mg (80%). Mp: 180 °C. Anal. Calcd for $C_{20}H_{23}IN_2O_4Pt$: C, 35.46; H, 3.42; N, 4.13. Found: C, 35.16; H, 3.39; N, 4.34. ^{1}H NMR ($CDCl_3$): δ (ppm) 8.09−8.02 (m, 3H; H$^{2',6',6}$), 7.06 (d, J = 2.3 Hz, 1H; H^3), 6.98 (d, J = 8.6 Hz, 2H; H$^{3',5'}$), 6.91 (dd, J = 8.5, 2.3 Hz, 1H; H^5), 5.55 (s, 1H; CH=C(CH$_3$)$_2$), 4.01 (s, 3H; OCH$_3$), 3.91 (s, 3H; OCH$_3$), 2.15 (s, 3H; CH$_3$CO), 2.11 (s, 3H; CH$_3$CO), 1.22 (s, 3H; CH$_3$Pt); $^3J(^{195}Pt-H_3)$ = 25 Hz; $^2J(^{195}Pt-H)$ = 65 Hz.

Colors, reaction times, yields, melting points, and analytical and ^{1}H NMR data for complexes **4b−d** are as follows.

[(L^b)Pt(acac)(CH$_3$)I], 4b: 50 equiv of CH$_3$I; brownish; 6 days; crystallization from *n*-hexane; yield 76 mg (75%); mp 133.8 °C. Anal. Calcd for $C_{30}H_{43}IN_2O_4Pt$: C, 44.07; H, 5.30; N, 3.43. Found: C, 43.70; H, 5.44; N, 3.71. ^{1}H NMR ($CDCl_3$): δ (ppm) 8.07−8.00 (m, 3H; H$^{2',6',6}$), 7.02 (d, J = 2.1 Hz, 1H; H^3), 6.95 (d, J = 9.1 Hz, 2H; H$^{3',5'}$), 6.88 (dd, J = 8.6, 2.1 Hz, 1H; H^5), 5.53 (s, 1H; CH=C(CH$_3$)$_2$), 4.17 (m, 2H; OCH$_2$), 4.04 (t, 2H; OCH$_2$), 2.14 (s, 3H; CH$_3$CO), 2.09 (s, 3H; CH$_3$CO), 1.21 (s, 3H; CH$_3$Pt); $^3J(^{195}Pt-H_3)$ = 30 Hz; $^2J(^{195}Pt-H)$ = 65 Hz.

[(L^c)Pt(acac)(CH$_3$)I], 4c: 50 equiv of CH$_3$I; yellow; 6 days; crystallization from acetone/methanol; yield 43 mg (52%); thermotropic behavior in Table 3. Anal. Calcd for $C_{43}H_{59}IN_2O_6Pt$: C, 50.54; H, 5.82; N, 2.74. Found: C, 50.65; H, 5.66; N, 3.56. ^{1}H NMR ($CDCl_3$): δ (ppm) 8.16 (d, J = 8.9 Hz, 4H; H$^{a',d',2',6'}$), 8.07 (d, J = 8.4 Hz, 1H; H^6), 7.34 (d, J = 8.9 Hz, 2H; H$^{3',5'}$), 7.05 (d, J = 2.3 Hz, 1H; H^3), 6.99 (d, J = 8.9 Hz, 2H; H$^{b',c'}$), 6.91 (dd, J = 8.4, 2.3 Hz, 1H; H^5), 5.54 (s, 1H; CH=C(CH$_3$)$_2$), 4.19 (m, 2H; OCH$_2$), 4.06 (t, 2H; OCH$_2$), 2.15 (s, 3H; CH$_3$CO), 2.09 (s, 3H; CH$_3$CO), 1.22 (s, 3H; CH$_3$Pt); $^3J(^{195}Pt-H_3)$ = 32 Hz; $^2J(^{195}Pt-H)$ = 64 Hz.

[(L^d)Pt(acac)(CH$_3$)I], 4d: 100 equiv of CH$_3$I; yellow; 5 days; crystallization from diethyl ether/petroleum ether; yield 41 mg (55%); thermotropic behavior in Table 3. Anal. Calcd for $C_{48}H_{59}IN_2O_8Pt$: C, 51.75; H, 5.34; N, 2.51. Found: C, 51.83; H, 5.30; N, 2.27. ^{1}H NMR ($CDCl_3$): δ (ppm) 8.27 (d, J = 8.6 Hz, 1H; H^6), 8.23 (d, J = 9.0 Hz, 2H; H$^{2',6'}$), 8.18 (d, J = 8.9 Hz, 2H; H$^{a',d'}$), 8.17 (d, J = 9.0 Hz, 2H; H^{a,d}), 7.47 (d, J = 2.3 Hz, 1H; H^3), 7.38 (d, J = 9.0 Hz, 2H; H$^{3',5'}$), 7.34 (d, J = 8.6 Hz, 2.3 Hz, 1H; H^5), 7.01 (d, J = 9.0 Hz, 2H; H$^{b',c'}$), 7.00 (d, J = 9.0 Hz, 2H; H^{b,c}), 5.57 (s, 1H; CH=C(CH$_3$)$_2$), 4.07 (t, 2H; OCH$_2$), 4.06 (t, 2H; OCH$_2$), 2.15 (s, 3H; CH$_3$CO), 2.11 (s, 3H; CH$_3$CO), 1.58 (s, 3H; CH$_3$Pt); $^3J(^{195}Pt-H_3)$ = 25 Hz; $^2J(^{195}Pt-H)$ = 63 Hz.

X-ray Structure Determinations of [(L^a)Pt(acac)], 2a, [(L^a)Pt(acac)I$_2$], 3a, and [(L^a)Pt(acac)(CH$_3$)I], 4a. Diffraction measurements were carried out on a Siemens R3m/V automated four-circle diffractometer equipped with graphite-monochromated Mo Kα radiation (λ = 0.710 73 Å). The data were corrected for Lorentz, polarization, and X-ray absorption effects, and an empirical absorption correction was applied using a method based upon azimuthal (Ψ) scan data.[33] Details of crystal data collection are listed in Table 4. The structures were solved by Patterson and Fourier methods and refined by full-matrix least-squares. The weighting scheme used in the last refinement cycle was $w^{-1} = \sigma^2|F_o| + q|F_c|^2$, with q = 0.0133 for complex **2a**, q = 0.0010 for complex **3a**, and q = 0.0020 for

(32) Ghedini, M.; Morrone, S.; Neve, F.; Pucci, D. *Gazz. Chim. It.* **1996**, *126*, 511.
(33) North, A. C. T.; Phillips, D. C.; Mathews, F. S. *Acta Crystallogr., Sect. A* **1968**, *24*, 351.

complex **4a**, respectively. All the non-hydrogen atoms were refined anisotropically, and the hydrogen atoms were included as idealized atoms riding on the respective carbon atoms with C−H bond lengths appropriate to the carbon atom hybridization. The isotropic displacement parameter of each hydrogen atom was fixed at $U = 0.08$ Å^2. Convergences for 3003, 3202, and 2077 observed reflections [$I > 2\sigma(I)$] and 235 and 253 parameters respectively for complexes **2a**, **3a**, and **4a** were reached at $R = 0.032$, 0.043, and 0.064, $R' = 0.040$, 0.047, and 0.071. All calculations were performed with SHELXTL PLUS[34] and PARST[35] programs. Atomic scattering factors were as implemented in the SHELXTL PLUS program.

Acknowledgment. The present work was supported by the Italian Ministero dell'Università e della Ricerca Scientifica e Tecnologica (MURST) and Consiglio Nazionale delle Ricerche (CNR).

Supporting Information Available: Atomic coordinates and U_{eq}, intramolecular bond distances and angles, hydrogen coordinates and isotropic displacement parameters, anisotropic displacement parameters for **2a**, **3a**, and **4a** (Tables S1−S12). This material is available free of charge via the Internet at http://pubs.acs.org.

OM9808155

(34) *SHELXTL PLUS*, Version 4.21; Siemens Analytical X-ray Instruments Inc.: Madison, WI, 1990.

(35) Nardelli, M. *Comput. Chem.* **1983**, *7*, 95.